ORIGINAL PAPER

Tree-ring-based temperature reconstruction since 1766 CE in the eastern Tianshan Mountains, arid Central Asia

Zhengbing Peng[1,2] · Li Qin[1] · Xinjian Li[1] · Heli Zhang[1] · Youping Chen[1,2] · Rui Liu[1,2] · Ruibo Zhang[1]

Abstract

Knowledge of past climatic variability in the eastern Tianshan Mountains of arid Central Asia is still limited due to the lack of long-term instrumental data. In this study, we develop a March–August mean temperature reconstruction since 1766 CE based on annual tree-ring widths of Schrenk spruce (*Picea schrenkiana* Fisch. et Mey.). The reconstruction accounts for 51.8% of the temperature variation during the calibration period (1957–2017). Over the last two and a half centuries, the region has experienced six warm periods, namely 1766–1792, 1803–1827, 1878–1886, 1904–1916, 1926–1935, and 1982–2015. The reconstruction also indicates the occurrence of two significant cold periods, 1821–1857 and 1931–1980. Over the past 252 years, the climate in this region has shifted between warm-dry and cold-wet periods. However, a strong warm-wet trend since the 1980s is evident. There is a strong positive correlation between the tree-ring temperature reconstruction and the North Atlantic Oscillation, as well as a close relationship with strong volcanic eruptions in the mid-high latitudes.

Keywords Tree rings · Schrenk spruce (*Picea schrenkiana* Fisch. et Mey) · Temperature reconstruction · Eastern Tianshan Mountains · Arid Central Asia

1 Introduction

According to the Fifth Assessment Report of the Intergovernmental Panel on Climate Change (IPCC), the mean global surface temperature has increased 0.85 °C (0.65–1.06 °C) over the last hundred years. Between 1951 and 2012, it increased to 0.12 °C/10a (0.08–0.14 °C/10a), an increase that is about twice as much as the increase since 1880. Climate change strongly affects ecological and social-economic systems (Houghton 2004), so it is imperative to understand the mechanisms of climate change in a given region. However, to understand long-term trends in climate, we need long-term records of climatic parameters, which are lacking in most parts of the world. Paleoclimatic proxies such as tree rings provide a means of extending the climate record into the past. Tree rings in many parts of the world can be accurately dated and provide long time series, strong continuity, wide spatial distribution, high resolution, and sensitivity to climate change. As a result, tree rings have become widely used proxies for studying paleoclimate change (Briffa et al. 2001).

The arid regions of Central Asia are ideal for tree-ring and climate research due to their harsh environments and sensitivity to climate change (Seddon et al. 2016). Because the region is severely lacking in instrumental data, proxy studies are especially important. In recent years, many studies (Zhang et al. 2016a, b, 2017a, b, 2019, 2020; Chen et al. 2016a, b, c) have used tree rings to understand climate change in the arid regions of Central Asia.

The Tianshan Mountains are a central feature of arid Central Asia because they are the main source of water for the whole region. These mountains are characterized by their deep inland location, temperate continental arid climate, and special biota and ecological processes (Chen et al. 2016a, b, c). Because of the extreme aridity of the region, the radial

✉ Li Qin
  Qinli@idm.cn

✉ Xinjian Li
  Lxj@idm.cn

1 Key Laboratory of Tree-Ring Physical and Chemical Research of China Meteorological Administration/Key Laboratory of Tree-Ring Ecology of Xinjiang Uigur Autonomous Region/Institute of Desert Meteorology, China Meteorological Administration, Urumqi 830002, China

2 College of Geographical Science and Tourism, Xinjiang Normal University, Urumqi 830054, China

growth of trees in Central Asian Mountains is likely to be more responsive to precipitation than to temperature, especially in areas below the tree line (Seim et al. 2015). The climate of the eastern Tianshan Mountains is more arid than that of the western and central Tianshan Mountains. The radial growth of Schrenk spruce (*Picea schrenkiana* Fisch. et Mey) growing in the eastern mountains is therefore expected to be more sensitive to changes in precipitation (Zhang et al. 2015). Moreover, the main economic activity in the region is agricultural production; the level of industrialization is low. The growth of Schrenk spruce is therefore minimally affected by human activities and better reflects climate change.

Many dendroclimatology studies in the eastern Tianshan Mountains have focused on the moisture factors, whereas few have attempted to reconstruct temperature. Due to the lack of research about past temperature changes here, the mechanisms of past changes are not well understood. Steinman et al. (2015) believed that the joint effect of the Northern Atlantic Oscillation (NAO) and the Interdecadal Pacific Oscillation (IPO) is primarily responsible for the temperature changes in the Northern Hemisphere. Some scholars have also found that natural forcing (especially NAO and volcanic activity) has an important impact on climate (Adams et al. 2003; Liu et al. 2013; Ning et al. 2018). In order to address this lack of information about long-term temperature trends in the eastern Tianshan Mountains, this study uses tree rings to reconstruct past temperatures. We also explore whether historical temperature changes are related to natural forcing (especially NAO and volcanic activity).

2 Data and methods

2.1 Study area and sample collection

The study area is located in the Hami area in the eastern part of the Tianshan Mountains. This is a topographically complex area, with alpine glaciers, forest canyons, and wetland meadows (Fig. 1). The sampling site is located at Lanqigou (LQS: 93° 20′ E, 43° 48′ N, 2443 m) in the Balikun Mountains (Fig. 1), far from human settlements. Samples of Schrenk spruce were collected following standard sampling procedures (Fritts 1976) in July 2017. In particular, trees growing close to the cliff edge and surrounded by sparse vegetation were sampled, as these trees are likely to be more strongly affected by climatic conditions. A total of 24 older live trees were sampled at breast height using increment borers, resulting in a total of 48 cores (2 per tree).

2.2 Development of the ring-width chronology

Following standard tree-ring analysis procedures (Fritts 1976), the sample cores were dried naturally, fixed to wooden

mounts, polished, and visually measured in the laboratory. The annual ring-widths were measured to an accuracy of 0.001 mm using the LINTAB program (Velmex Measuring System). The COFECHA program was employed to carry out quality control of the cross-dating (Holmes 1983). Finally, the ARSTAN program was used to establish the tree-ring chronology (Cook and Krusic 2007). The negative exponential function method was applied to remove the growth trend, and the de-trending sequence was synthesized by the double-weighted mean method to obtain the standard chronology (STD), the residual chronology (RES), and the autoregressive chronology (ARS). This paper uses the LQS standard chronology, as it contains more low-frequency information.

The Rbar weighted method was used to stabilized the variance of the chronology (Cook and Krusic 2007) (Fig. 2b). Then, we used the expressed population signal (EPS) to determine a common period for the individual chronologies (Cook and Kairiukstis, 1990). To maximize the length of the tree-ring chronologies and ensure the reliability of the reconstruction, we restricted our analysis to the period with an EPS of at least 0.85 (Wigley et al. 1987). Thus, the reliable LQS chronology spans the period 1766–2017 (Fig. 2b). It is generally believed that a high-quality chronology is characterized by a higher mean sensitivity, a higher standard deviation, and a higher signal-to-noise ratio. The mean sensitivity of the LQS standard chronology is 0.323, the standard deviation is 0.354, and the signal-to-noise ratio is 67.282 (Table 1). Thus, this chronology can be expected to contain reliable climate information.

2.3 Meteorological data

Mean monthly temperature and precipitation data for this study were obtained from the Balikun meteorological station (93° 0′ E, 43° 36′ N, 1650.9 m, 1957–2015), which is closest to the LQS site and located in a similar habitat (Fig. 1). The instrumental records originate from the China Meteorological Data Sharing Service System (http://cdc.cma.gov.cn/). These data indicate that high temperatures from June to August coincide with increased precipitation in this region (Fig. 3a). Summer is the high-temperature period, with the highest mean temperature occurring in July. Rainfall from June to August comprises a significant proportion of the annual total precipitation (53%) and peaks in July. The instrumental data show a significant ($p < 0.01$) increase in temperature that begins in the early 1980s. Precipitation has increased over the same period ($p < 0.01$) (Fig. 3).

2.4 Analysis methods

Because the first-order autocorrelation of the LQS chronology is 0.537 (Table 1), it can be assumed that the lagging response

Fig. 1 Location of the tree-ring sampling sites and the meteorological station in the eastern Tianshan Mountains
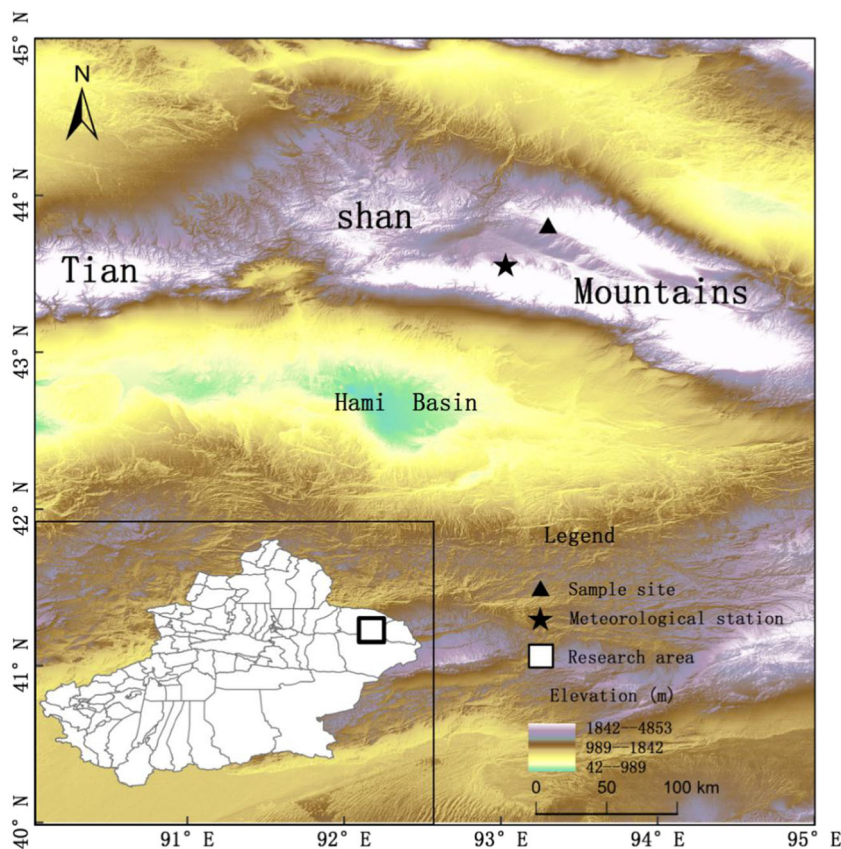
of tree growth in response to climate is taken into account (Joel 1987). We screened the LQS chronology using a Pearson correlation analysis with climate data spanning from previous October to current September.

Based on the correlation between tree-ring width and observed temperature data, we established a temperature reconstruction equation from the mean March–August temperature

and the LQS chronology. Due to the limited temporal coverage of the calibrated meteorological device (1957–2015), the reliability of the reconstruction equation was tested with the leave-one-out, or jackknife method (Joel 1987). Originally proposed by Maurice Quenouile in 1949, the basic idea is to remove the first sample in the set, reconstruct the regression coefficient of the conversion function with the remaining

Fig. 2 a The LQS chronology (thin line) and sample depth (dashed line). **b** The EPS (thick line), the Rbar (thin line), EPS = 0.85 threshold (dashed line), and the mean Rbar (dotted line)
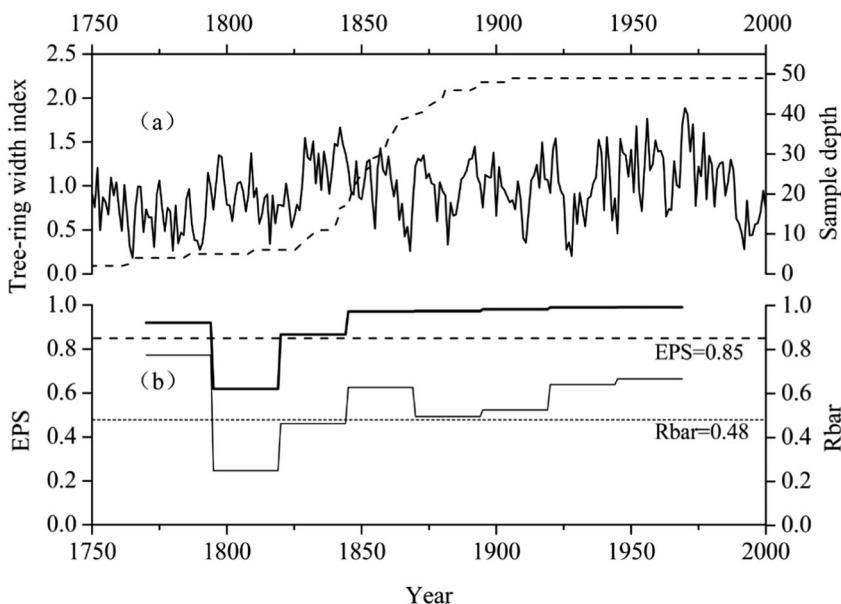
Table 1 The statistical characteristics of the standard LQS chronology

Statistic	STD
Time period	1712–2017
Mean	0.93
Mean sensitivity (MS)	0.323
Standard deviation (SD)	0.354
Kurtosis coefficient (K)	2.862
Skewness coefficient (S)	0.268
First-order autocorrelation	0.537
Mean correlation within a tree ($r1$)	0.887
Mean correlation between trees ($r2$)	0.593
Signal-to-noise ratio (SNR)	67.28
Expressed population signal (EPS)	0.985
variance in the first principal comment (PC1)	0.616
Begin year of EPS > 0.85	1766

Fig. 4 Pearson correlations between the tree-ring width chronology and the meteorological data (precipitation, mean temperature). The blue bars represent monthly precipitation totals (in mm) and the green bars represent monthly mean temperatures (in °C). P10, P11, and P12 represent October, November, and December of the previous year, respectively. C1–C9 are the January, February, March, April, May, June, July, August, and September of the current year, respectively. C3–8 indicates the mean from March to August of the current year. The blue dashed line represents a 0.05 significance level. The red dashed line represents a 0.01 significance level

samples, and estimate the first reconstruction target value, then reject it in turn. Finally, the statistical parameters are obtained (Holder et al. 1979). The statistical parameters include the correlation coefficient, the F value, the reduction of error, and the explained variance (Cook and Kairiukstis 1990). To test the stability of the reconstructed equation, we also compared the reconstructed and the measured values, as well as their first-order differences (Fig. 4). We used CRU March–August mean temperature data from 1957 to 2015 as the verification period and conducted a Pearson correlation analysis with the reconstruction.

To determine the representativeness of the reconstruction series on a larger spatial scale, we used the mean March–August temperature from 1957 to 2015 from CRU TS4.03 grid data (http://climexp.knmi.nl; 0.5° × 0.5°) and carried out a spatial correlation analysis with the reconstruction using the KNMI Climate Explorer (Trouet and Oldenborgh 2013). In addition, we applied a power spectrum analysis to examine the reasonable periodicities in our reconstruction.

To explore the regional representation of the reconstructed series, we compared it with two previous temperature
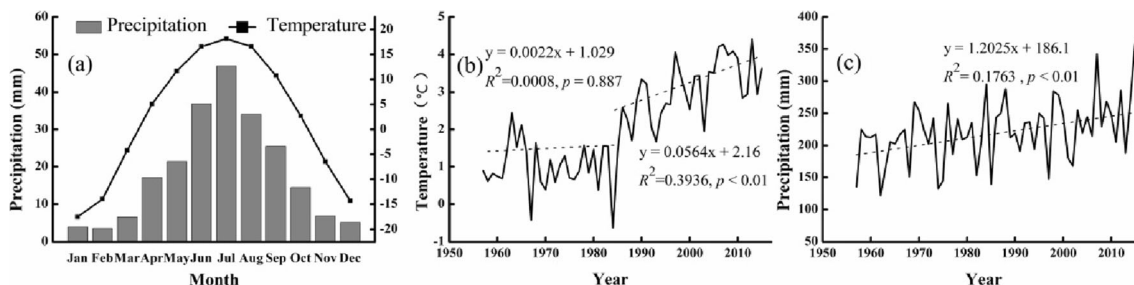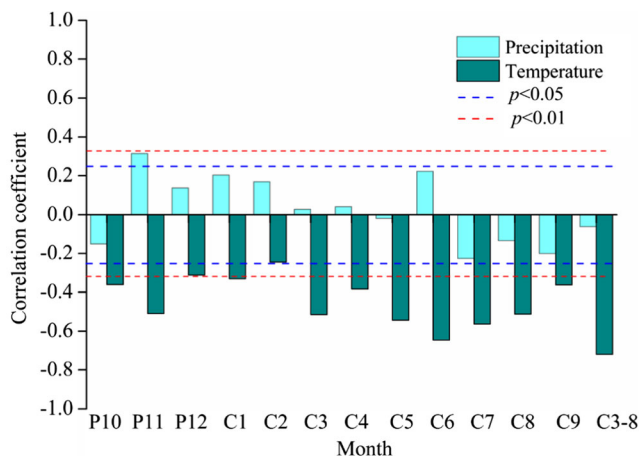
reconstructions for Central Asia (Jiang et al. 2016; Chen et al. 2017). Furthermore, to explore past climate patterns in the study area, we compared the precipitation reconstruction of Zhang et al. (2015) with that of this paper.

Hurrell (1995, 1996) pointed out that the recent increase in temperature in Eurasia, as well as the mean temperature change in the mid-high latitudes of the Northern Hemisphere, can be explained by the NAO. To study the effect of the NAO on mean March–August temperature in the eastern Tianshan Mountains, we computed the spatial correlation between the reconstructed mean March–August temperature and HadISST1 1° (Rayner et al. 2003) over the 1957–2015 period.

Volcanic activity is also known to cause interannual and interdecadal variations in global climate (IPCC 2013). Previous studies have shown that tree-rings in most parts of the Northern Hemisphere are affected by volcanic activity.

Fig. 3 Climatic diagram for the Balikun meteorological station in the eastern Tianshan Mountains, northwestern China (1957–2015). **a** Bars indicate monthly precipitation totals (mm), and the curve indicates monthly mean temperatures (°C). **b** Annual mean temperature (solid line) and trend line for the annual mean temperature for the period 1957–2015 (dashed line). **c** Annual precipitation totals (solid line) and trend line for the annual precipitation totals for the period 1957–2015 (dashed line)

Summer temperatures tend be lower for 1–2 years following strong volcanic eruptions (Miller et al. 2012), resulting in less tree growth (Briffa et al. 1998). To study the effect of volcanic eruptions on tree growth in the eastern Tianshan Mountains, we identified major eruptions using the Volcanic Explosivity Index (VEI) series shared by the Smithsonian Volcano Institute (http://volcano.si.edu). Over the past 252 years, there have been ten strong volcanic eruptions with a VEI ≥ 5. We then used Superposited Epoch Analysis (SEA, Schoennagel et al. 2005) to study the effect of volcanic eruptions on temperature.

3 Results

3.1 Growth-climate responses

The LQS chronology is weakly correlated with precipitation (Fig. 5), but significantly ($p < 0.01$) and negatively correlated with the mean temperature in October of the previous year and in March, May, June, and July of the current year. The highest negative correlation ($r = -0.646$) occurs during June of the

current year and is most strongly correlated with the mean temperature from March to August of the current year ($r = -0.72$, $p < 0.01$, $n = 58$).

3.2 Temperature reconstruction and inspection

The March–August mean temperature reconstruction equation for the full calibration period (1957–2015) is:

$$T_{3-8} = -2.177 \text{LQS}_{std} + 12.721 \tag{1}$$

In Eq. (1), T_{3-8} is the mean temperature from March to August, and LQS_{std} is the standardized Lanqigou chronology. The results (Table 2) show that the reconstruction equation correlation is 0.761, the significance level test reaches 0.001, the explained variance is 51.8%, and the explained variance after adjusting for the loss of degrees of freedom is 50.9% (Table 2). The product mean test is 7.65, passing the 0.001 significance level. The F value is 60.16 ($p < 0.01$); the first-order difference symbol test also passes the 0.01 significance level. The reduction of error is high and positive at 0.49, so the detection data can be considered to be reliable. These statistics indicate that the reconstruction equation is reliable. The
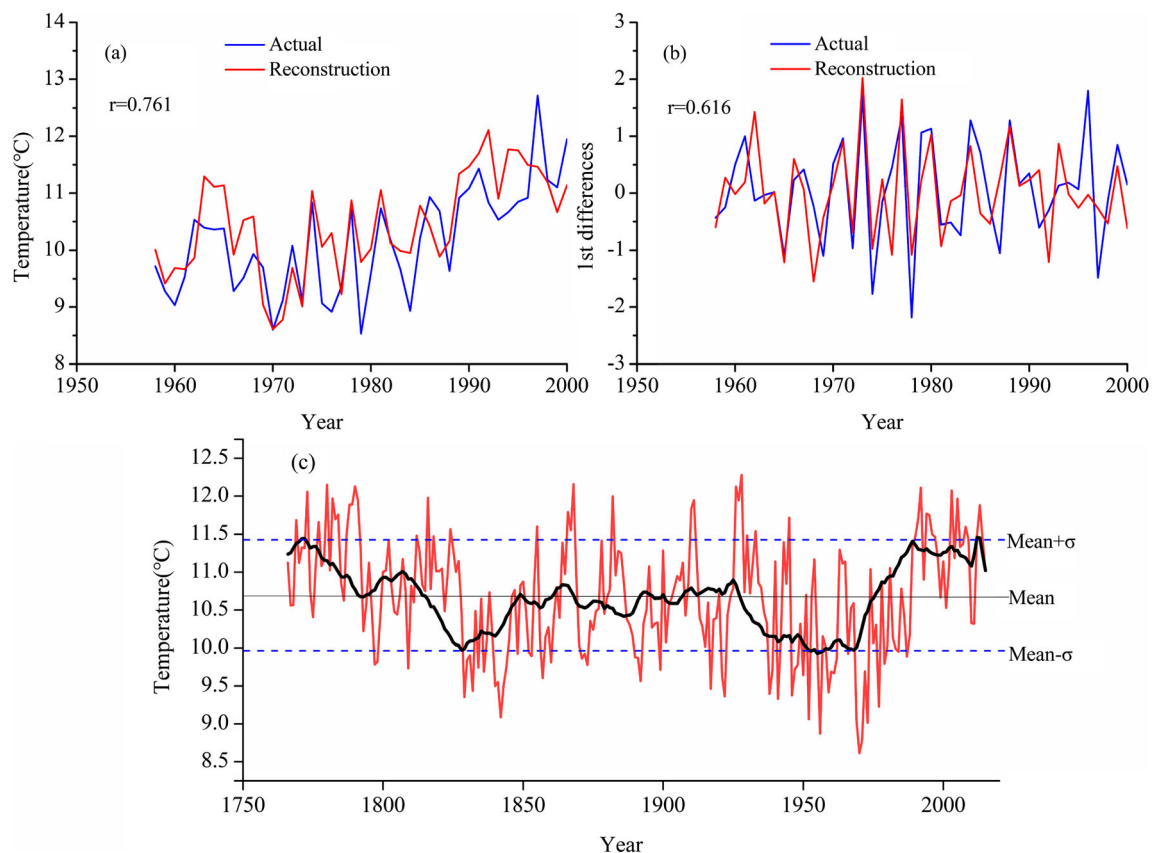

Fig. 5 **a** Comparison of the mean temperature reconstruction (red line) and the observed data (blue line). **b** The first-order difference of the mean temperature reconstruction (red line) is compared with the first-order difference of the observed data (blue line). **c** The March–August mean temperature reconstruction in the Balikun area of the eastern Tianshan Mountains since 1766 C.E. (red thin line). The thick line shows the smoothed data with an 11-year low-pass filter to emphasize the long-term fluctuations. The solid horizontal line represents the long-term mean for the 1766–2017 period. The blue dashed horizontal lines represent the mean ± σ

Table 2 Statistical parameters of the transfer function and cross-validation

R^2	R^2_{adj}	First-order sign test	Sign test	t	F	RE	Correlation coefficient with CRU (1957–2015)
51.8%	50.9%	40+/17−*	47+/11−*	7.65	60.16	0.49	0.513

R^2, the Explain variance; R^2_{adj}, the explained variance after adjustment for the loss of degrees of freedom; t, the product mean test; F, the F value; RE, the reduction of error

*Significance at the 99% level of confidence

correlation coefficient between the reconstructed and the observed values is 0.76, and the correlation coefficient of their first-order difference is 0.62.

The correlation coefficient between the reconstruction and the CRU temperature date is 0.513 ($p < 0.01$, $n = 59$), indicating that the reconstruction equation is both accurate and stable. This equation is therefore used in this study to reconstruct the mean growing season temperature in the eastern Tianshan Mountains over the past 252 years.

3.3 Characteristics of the reconstructed temperature series

The mean value of the reconstruction series is 10.69 °C and the standard deviation (σ) is ±0.76 °C. We define a high temperature year as > mean + σ and a low-temperature year as mean σ (Fig. 6). Over the entire reconstruction series, the annual high-temperature ratio is 16.2%, the low-temperature ratio is 19.8%, and the normal temperature ratio is 64%. The three hottest years occurred during the twentieth century: 1926, 1928, and 1992. The three lowest temperatures were 1950, 1970, and 1971. Over the last two and a half centuries, the region has experienced six warm periods, namely 1766–1792, 1803–1827, 1878–1886, 1904–1916, 1926–1935, and

1982–2015. The reconstruction also indicates the occurrence of two significant cold periods, 1821–1857 and 1931–1980. From the Industrial Revolution in the 1860s to the beginning of the twentieth century, the mean temperature has been above average. From the 1950s to the 1980s, the mean temperature was below average. Since the 1980s, it has risen continuously. The past 30 years represent the warmest period of the past three centuries.

The spatial correlation results of the reconstruction in this paper and the observation records are similar (Fig. 6). It is also representative of Central Asia, including the northern part of Xinjiang and parts of eastern Kazakhstan and western Mongolia (Fig. 6). Thus, the reconstructed temperature signal is representative not just of the eastern Tianshan Mountains in Xinjiang but also of a large part of Central Asia.

Multi-window power spectrum (MTM) analysis shows that the reconstruction series has 69.6-, 12-, 9.8-, 2.3-, and 2.1-year quasi-periodic oscillations at the 95% confidence level (Fig. 7). The 2.1–2.3-year cycle coincides with a regular cycle in the Tianshan Mountains that may be related to the Quasi-Biennial Oscillation (QBO). The 9.8- and 12-year cycles are similar to the solar activity quasi-period. The 69.6-year cycle may be related to the irregular oscillation of the North Atlantic thermohaline circulation.
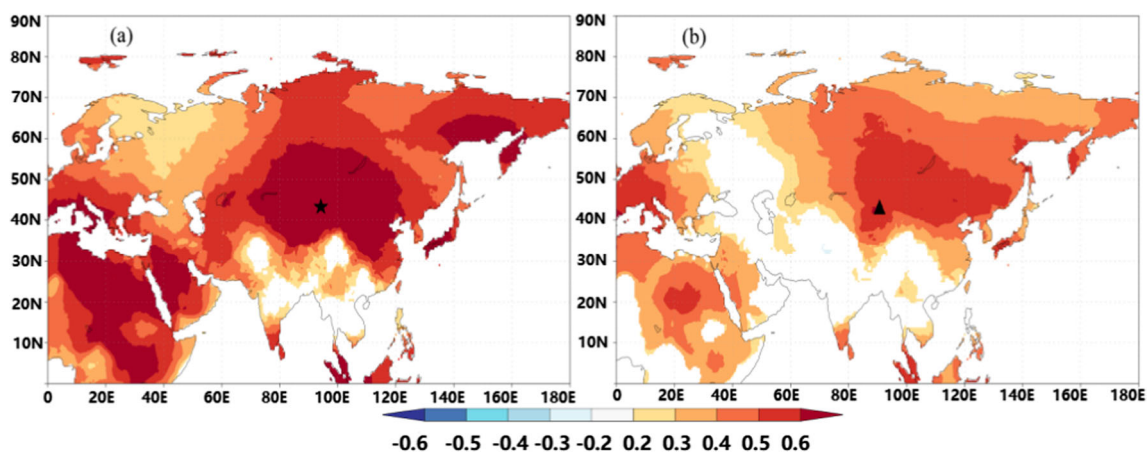

Fig. 6 a Spatial correlations between the gridded dataset of surface temperatures (March–August) and the observed temperatures (March–August) at the Balikun meteorological station. The black star indicates the location of the meteorological station. **b** Spatial correlations between the gridded dataset of surface temperatures (July–August) and the temperature reconstruction for the eastern Tianshan Mountains. Analyses were performed using the KNMI Climate Explorer (http://climexp.knmi.nl). The black triangle indicates the sampling site location
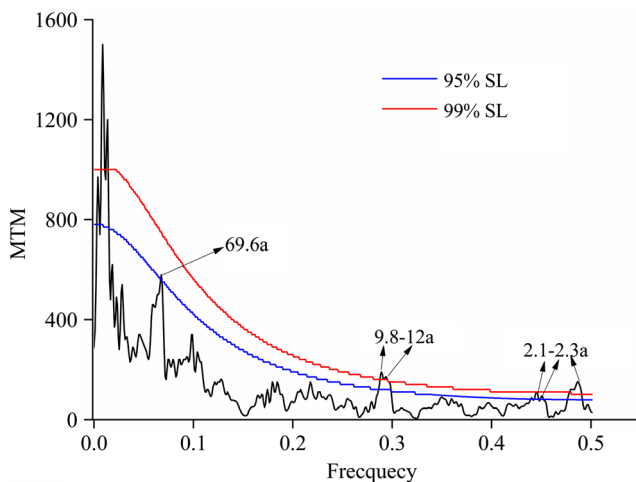
Fig. 7 Results of the MTM spectrum analysis of the reconstruction. The red line represents a red noise significance level of 99%. The blue line represents a significance level of 95%

4 Discussion

4.1 The dendroclimatological potential of Schrenk spruce

This study, like many others (Schweingruber et al. 1978; Hughes et al. 1984; Briffa et al. 1992; Brauning and Mantwill 2004; D'Arrigo et al. 2005), reconstructs temperature using tree-ring widths of Schrenk spruce. Other studies have used Schrenk spruce to reconstruct temperature elsewhere in the region, including in the western Tianshan Mountains (Zhang et al. 2020), the Kunlun Mountains in Xinjiang (Huang et al. 2019), and on the Tibetan Plateau (Zhu et al. 2011). In the Tianshan Mountains, the radial growth of trees near the lower tree-line is limited by moisture (Zhang et al. 2016a, b), but the relationship between growth and climate is more complex at higher elevations.

The LQS chronology is not sensitive to precipitation. It is likely that the sampling site (2443 m a.s.l.) receives enough precipitation to support tree growth and that precipitation is therefore not a limiting factor. Most other studies of tree growth and precipitation in the Tianshan Mountains have focused on lower-elevation sites (Table 3) where precipitation may be more limited. In addition, trees at higher elevations respond to changes in the ecological environment by lowering their metabolism and are thus less sensitive to changes in the environment (Splechtna et al. 2000). The radial growth of tree rings at the study site is negatively correlated with temperature, which is a common phenomenon in the arid and semi-arid areas of northwestern China (Jiao et al. 2016; Zhang et al. 2016a, b). According to the correlation analysis, the mean March–August temperature is the main factor limiting tree growth in this area.

Schrenk spruce grows according to the following timeline: in March, temperatures rise rapidly and soil moisture

evaporates quickly. From April to May, temperatures continue to rise, leading to moisture evaporation and plant transpiration, as well as to an intensification of the direct consumption of nutrients. From June to July, a key period for the formation of early wood, Schrenk spruce enters a period of rapid growth (Cai et al. 2013; Liang et al. 2009). This is also the warmest part of the year; warmer temperatures result in a sharp decrease in effective moisture, which can lead to the formation of a narrow ring if too little moisture is available. In August, the tree enters the late growth stage. At this time, the growth of trees has not stopped, so suitable temperatures promote the formation of rings. In the eastern Tianshan Mountains, tree growth is affected primarily by moisture scarcity caused by high temperatures or drought stress (Chen et al. 2016a, b, c; Jiao et al. 2016; Zhang et al. 2016a, b).

To further examine the effect of drought on tree growth, we compared the standardized LQS chronology with the Palmer Drought Severity Index (PDSI) (Dai et al. 2004). We found that the correlation between the chronology and the PDSI was not significant in each month. This may be due to the high density of the forest canopy (0.5) or to the relatively thick, moisture-rich soils, either of which might obstruct proper PDSI readings.

4.2 Regional climate comparison

There is significant consistency between the reconstruction described in this paper, the reconstruction of Chen et al. (2017), and the reconstruction of Jiang et al. (2016) (Fig. 8). This consistency implies a common forcing factor. Tropical volcanoes occurred regularly during the early nineteenth century, and multiple studies have shown that volcanic eruptions can cause a significant drop in summer temperatures (Chenoweth 2001; Chen et al. 2019; Miller et al. 2012). Following the "Year of No Summer" in 1816 (Matsikaris et al. 2016), the temperature in the study area exhibits a relatively significant downward trend. This trend corresponds with that observed by Chen et al. (2017) in northern Xinjiang. Around the middle of the nineteenth century, the three reconstructions (this paper; Jiang et al. 2016; Chen et al. 2017) experience a period of "cooling-heating-cooling", the summer temperatures (Shang et al. 2011; Chen et al. 2012; Zhang et al. 2020) reconstructed in Central Asia, which also showed the same fluctuations during the same period. During the first half of the twentieth century, the reconstruction in this paper indicates generally higher temperatures, a result that is consistent with summer temperature reconstructions for northern Xinjiang and Central Asia (Shang et al. 2011; Chen et al. 2017; Jiang et al. 2016). The reconstruction of this paper and the northern Xinjiang series of Chen et al. (2017) show a significant warming trend after the 1980s, consistent with the global warming trend. This indicates that the eastern Tianshan Mountains are responsive to global warming.

Table 3 Information about previous dendroclimatology studies in the Tianshan Mountains

	Research area	Species	Tree ring and climate	Altitude	Source
Western Tianshan (Central Asia)	Southern Kazakhstan	Schrenk spruce	Precipitation reconstruction	1850 m	Zhang et al. 2016a, b
	Issyk-Kul Lake of Kyrgyzstan	Schrenk spruce	Precipitation and SPEI reconstruction	2200 m	Zhang et al. 2016a, b
	Sarekungey of Kyrgyzstan	Schrenk spruce	PDSI reconstruction	1630–1865 m	Chen et al. (2013)
Central Tianshan (China)	Hutubi River Basin	Schrenk spruce	PDSI reconstruction	1630–1865 m	Chen et al. (2015)
	Gongnaisi	Schrenk spruce	Precipitation reconstruction	2242 m	Shang et al. (2010)
	Urumqi River	Schrenk spruce	Precipitation reconstruction	2070 m	Yuan et al. (2002)
Eastern Tianshan (China)	Mulei	Schrenk spruce	Precipitation reconstruction	2285 m	Zhang et al. (2015)
	Mulei	Schrenk spruce	SPEI reconstruction	2000–2390 m	Chen et al. (2016a b, c)
	Balikun	Schrenk spruce	Temperature reconstruction	2443 m	This article

However, Jiang et al. (2016) reconstructed early summer temperatures in the Altai Mountains of Xinjiang for the period 1579–2009, but did not find a significant upward trend during this period. This may be because the temperature increase in this area mainly occurs in autumn and winter (Shang et al. 2011). The reconstruction of this paper is in significant agreement with temperature reconstructions from surrounding studies, indicating the reliability of our reconstruction and its representativeness of the arid regions of northern Xinjiang and Central Asia.

There is a negative correlation (− 0.23, $p < 0.01$) between the series described in this paper and that of Zhang et al. (2015) (Fig. 9). Over the past 20 years, the study area has experienced a warming-wetting trend (Fig. 9). Chen et al. (2017) found a similar warm-wet trend in the northern mountainous areas of Xinjiang, which is consistent with the available meteorological data (Fig. 3). This is likely related to the fact that the NAO entered an abrupt positive phase in the early 1980s (Fig. 10b). Temperature and precipitation reconstructions by Zhang et al. (2003) and Liu (2006) and Liu et al. (2009) for the Qaidam Basin show a similar warming-wetting trend.

Finally, we found a one-to-one correspondence between the warm-dry climate and the drought period of the SPEI reconstruction (Chen et al. 2016a, b, c) (Fig. 9). We found that the most severe drought period occurs in the warm-dry period, indicating that the drought is caused by a combination of high temperatures and low precipitation. For example, the droughts in 1805–1820, 1854–1868, 1875–1882, and 1906–1912 (Fig. 9a) during the warm-dry period correspond to the

Fig. 8 Comparison between this reconstruction and reconstructions from elsewhere in the region. **a** The reconstruction from this study, **b** a reconstruction for the northern part of Xinjiang (Chen et al. 2017), and **c** a reconstruction for the Altay (Jiang et al. 2016)
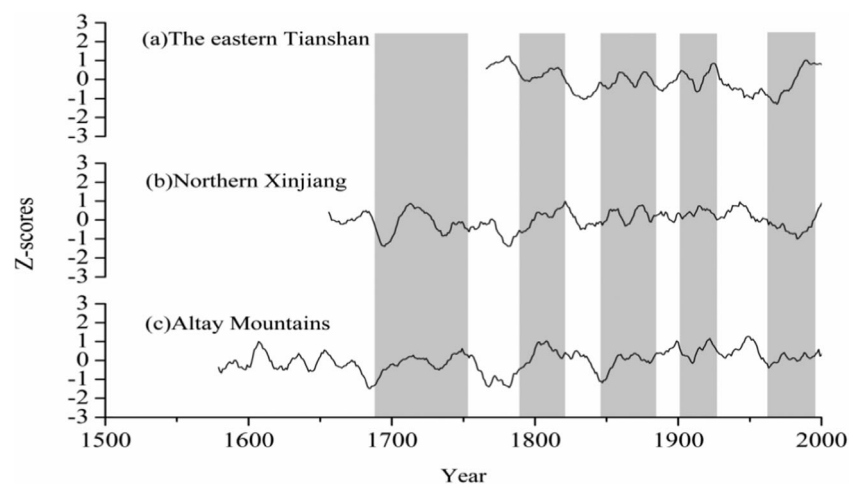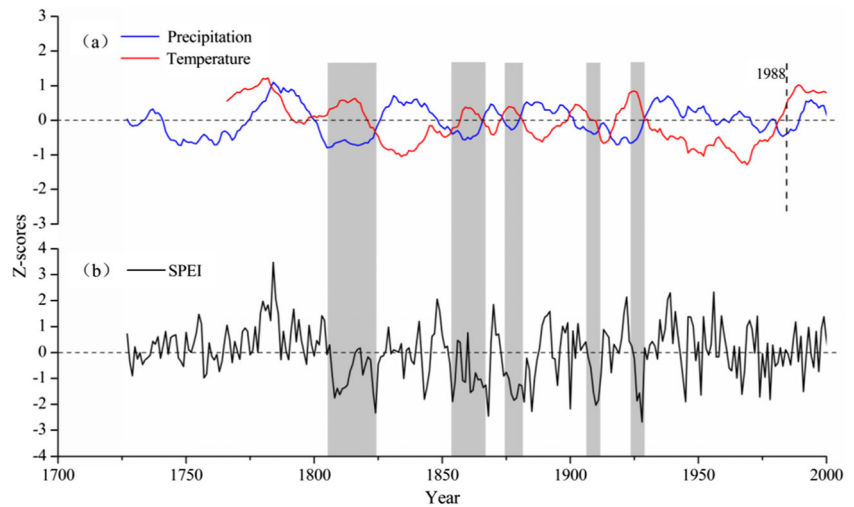
Fig. 9 **a** Comparison between temperature series (this study) and precipitation series (Zhang et al. 2015) in the eastern Tianshan Mountains. **b** The SPEI reconstruction series (Chen et al. 2016a, b, c) in the eastern Tianshan Mountains. The vertical dotted line indicates the beginning year of a period of warming and wetting


dry periods in the SPEI series: 1805–1828, 1853–1887, and 1905–1914 (Fig. 9b), respectively. Of these periods, 1924–1928 includes the driest year (1928) in the SPEI series, which shows that once the climate of the eastern Tianshan Mountains becomes warm and dry, drought may occur or worsen.

4.3 Connection between the reconstruction series and the NAO

The reconstruction correlates significantly with sea surface temperatures (SST) (Rayner et al. 2003) of the North Atlantic Ocean at mid-high latitudes (Fig. 10a). This suggests

Fig. 10 **a** Spatial correlation between the reconstructed mean March–August temperature during 1957–2015 in the Balikun area of the eastern Tianshan Mountains and HadISST1 1° (Rayner et al. 2003). **b**, **c** Graphical comparison of the reconstructed temperature in the Balikun area of the eastern Tianshan Mountains since 1766 with three winter NAO indexes. The green line shows the pattern-based NAO index for the period 1950–2011 (Climate Prediction Center; http://www.cpc.noaa.gov/date/teledoc/telecontents.shtml). The blue line indicates the reconstructed NAO index based on observations for the period 1865–2000 (Jones et al. 1997). The black line shows the reconstructed NAO index based on tree-ring data for the period 1049–1995 (Trouet et al. 2009)
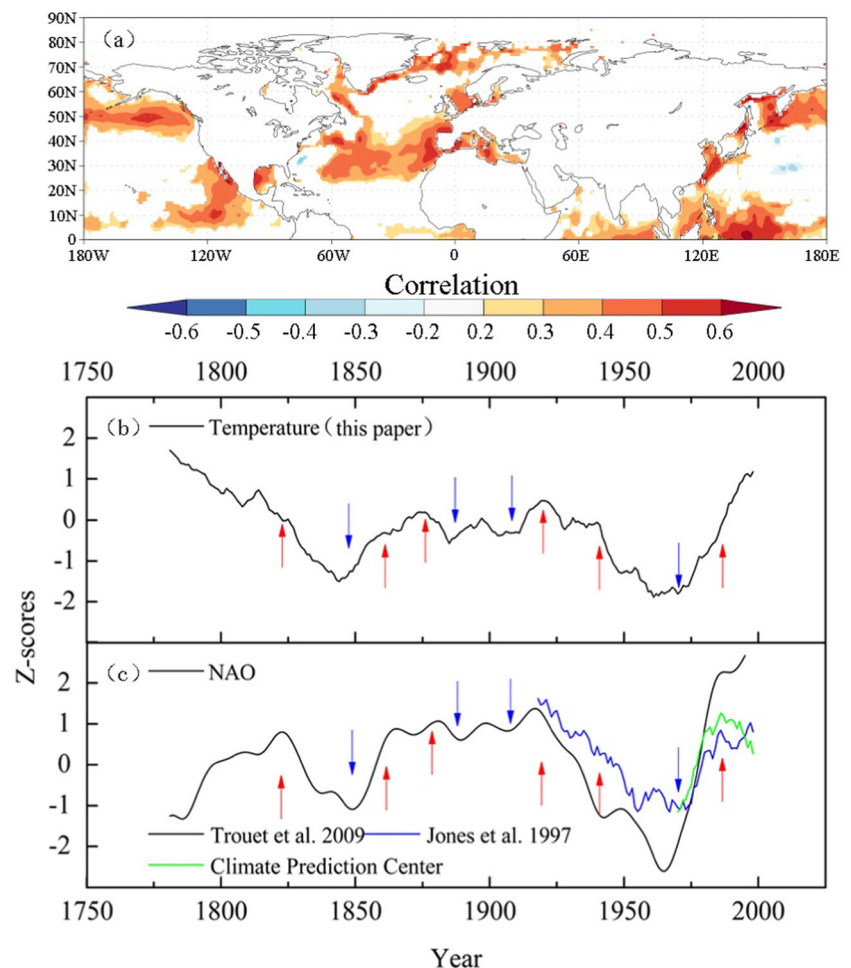
that the climate of Central Asia may be influenced by that of the Atlantic Ocean (Hurrell 1995). There is a significant coupling relationship between the North Atlantic SST and the NAO (Rodwell et al. 1999; Robertson et al., 2000). The correlation between the mean temperature series and the observed winter NAO (Climate Prediction Center; http://www.cpc.noaa.gov/date/teledoc/telecontents.shtml) is 0.618 ($p < 0.01$, $n = 41$). The correlation between the mean temperature series and the recorded winter NAO (Jones et al. 1997) is 0.82 ($p < 0.01$, $n = 107$). The correlation between the mean temperature series and the winter NAO reconstructed from tree rings (Trouet et al. 2009) is 0.73 ($p < 0.01$, $n = 196$) (Fig. 10b, c).

Large-scale climate trends are influenced not only by internal variability but also by frequent volcanic eruptions. This is especially true of the Laki (Schmidt et al. 2011) and Tambora (Chenoweth 2001) eruptions. Following these events in the early 1980s, the winter NAO rapidly entered a positive phase, possibly driving the switch to a warm-wet phase in the study area during the same time period. On the whole, the temperature reconstruction of this paper is in significant agreement with the winter NAO trend. Hao et al. (2011) suggest that the NAO has a significant impact on annual temperature in the western part of northern Xinjiang. It is possible that changes in the NAO drive changes in the atmospheric circulation system, which further promote changes in the westerly ridge system. The climate in Xinjiang and hence the eastern Tianshan Mountains is controlled mainly by the westerly circulation. Fu and Zeng (2005) found that summer drought and flooding in northern China and the whole eastern region have a lag relationship of 1–3 years with the winter NAO. Xin et al. (2006) suggested that spring climate anomalies in southern China are significantly correlated with winter NAO. In addressing the lag between the NAO and local climate, Gray (1998) proposed that the North Atlantic thermohaline circulation, which is closely related to NAO, may promote oceanic surging in the eastern hemisphere. This in turn causes an energy accumulation in the western Pacific warm pool area, resulting in El Niño changes. This begs the question of whether a similarly slow process causes the winter NAO teleconnection to influence the mean March–August temperature in the eastern Tianshan Mountains. Interestingly, we found that the reconstruction in this study is significantly correlated with mid-high latitude Pacific and Atlantic SSTs, and that the overall relevant sea area is connected to the westerly circulation belt (Fig. 10a). The potential relationship between the winter NAO and spring-summer temperatures in this area requires further study.

The existence of high frequency variation periods of 2.1 to 2.3 and 9.8 years are observed in the reconstruction in this paper. These cycles are also referred to in studies of interdecadal climate change and the North Atlantic Oscillation (Hurrell and Loon 1997). They are also very similar to the 2- to 4-year and the 7- to 8-year cycles of the NAO

index series reconstructed by Cook et al. (2002) using a variety of proxy data. These similar periodic correlations show that this reconstruction contains rich information about variations in the NAO, and that the NAO positively affects temperature in the study area. Moreover, the periods of 2.1 to 2.3 and 9.8 years imply that the temperature changes in the study area may also be related to the Pacific Decadal Oscillation (PDO; Fig. 10a; Chen et al. 2012).

4.4 Connection between the reconstruction series and strong volcanic eruptions

Our analysis reveals a significant drop in mean temperature in the eastern Tianshan Mountains in the third year after strong volcanic eruptions (Fig. 11b). Chen et al. (2017) compared a historical record of volcanic eruptions with a tree-ring density reconstruction series for Central Asia and found that temperatures in the second year following a major volcanic eruption were 0.4 °C lower than the mean value of the reconstruction. Strong volcanic eruptions occurring at low latitudes were also found to cause cooling in the eastern Tianshan Mountains, but the correlation does not reach a 95% significance level (Fig. 11a). Temperatures drop most significantly in the third year following an eruption, reaching a 95% confidence level. After this point, the influence of the eruption on climate gradually diminishes (Fig. 11b). In studying the impact of volcanic eruptions on China's climate over the past 50 years, Jia (2001) found that a 3-year lag between the time of the eruption and its observed influence on temperatures in China. Additionally, Shi et al. (2015) used an integrated tree-ring reconstruction to analyze the mean annual temperature change following strong volcanic eruption in the Northern Hemisphere over the past 2000 years. They found that the impact of volcanic
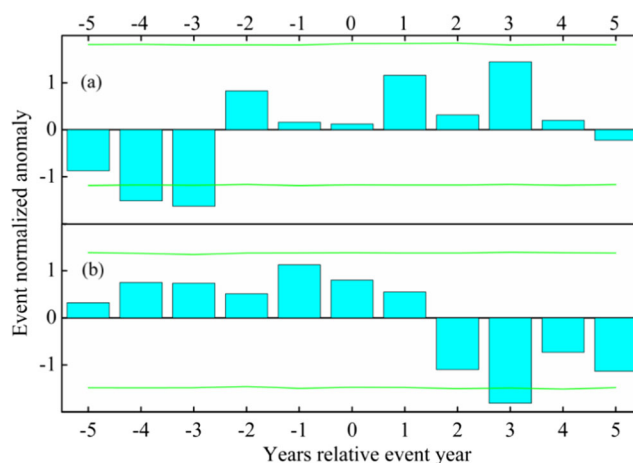

Fig. 11 Superposed epoch analyses center on ten large volcanic eruptions (VEI ≥ 5) that have occurred in the past 252 years. **a** The effect of a strong volcanic eruption at 10° S–30° N on temperature in the eastern Tianshan Mountains, Xinjiang. **b** Influence of a strong volcanic eruption north of 30° N on temperature in the eastern Tianshan Mountains, Xinjiang. The green line represents a 95% confidence level

eruptions on temperature is similar to that observed in this study. It is common for volcanic eruptions to affect temperatures, as previous studies have shown (Briffa et al. 1998; Man et al. 2014).

The mechanism by which a strong volcanic eruption affects temperature (Robock 2000) is that a large amount of sulfur gases is entrained in the atmosphere to form sulfate aerosols, which attenuate solar radiation and thereby reduce surface temperatures (D'Arrigo and Jacoby 1999). Robock (2000) noted that strong volcanic eruptions affect a wide range of climate systems, such as the air-sea cycle, causing surface temperature changes. Using tree rings, Chen et al. (2016a, b, c, 2017) discussed the impact of the 1783 Icelandic Laki eruption on temperature in northern Xinjiang and northeastern Kazakhstan. They identified 1783 as the coldest year, but our reconstruction suggests that 1786 was the coldest year (Fig. 11b). This difference is likely due to the fact that the impact of volcanic eruptions depends on the timing of the eruption, the regional climate, etc. (D'Arrigo and Jacoby 1999; D'Arrigo et al. 2013; Robock and Mao 1992). Esper et al. (2013) also found geographical differences in the impact of strong volcanic eruptions on European temperatures.

The westerly circulation dominates the climate of Xinjiang. As a result, aerosols formed by volcanic ash are likely to accumulate first in the upper North Atlantic and then be transported to western Siberia and Xinjiang by the downstream westerly circulation (Chen et al. 2017; Schmidt et al. 2011). It is also possible that volcanic eruptions affect the current of the North Atlantic Ocean (D'Arrigo and Jacoby 1999), resulting in changes in sea surface temperatures that then affect the surrounding air masses.

5 Conclusions

This study provides further evidence that the growth of Schrenk spruce in the eastern Tianshan Mountains of Xinjiang is significantly influenced by mean March to August temperatures. The region has experienced six warm periods over the past 252 years: 1766–1792, 1803–1827, 1878–1886, 1904–1916, 1926–1935, and 1982–2015. The reconstruction also indicates the occurrence of two significant cold periods, 1821–1857 and 1931–1980. These results are in agreement with previous studies in northern Xinjiang. The observed warming trend since the 1980s is consistent with the global trend. Over the past 252 years, the climate in the eastern Tianshan Mountains has shifted between periods of warm-dry and cold-wet. For the past 20 years, the region has experienced a warming-wetting trend. The observed periods of 69.6, 9.8–12, and 2.1–2.3 years indicate that temperature changes in the eastern Tianshan Mountains are affected by both internal and external factors. There is a strong positive correlation between the reconstruction series and the winter

NAO. The fluctuation of the NAO in winter may affect temperatures in the eastern Tianshan Mountains in Xinjiang as a result of westerly circulation. However, the specific physical mechanism needs further exploration.

With regard to the influence of volcanoes on climate, the tree-ring record indicates that temperatures in the eastern Tianshan Mountains decline in the 1–3 years following major eruptions. This decline occurs most strongly during the second year, reaching a 95% confidence level. The climate of this region is primarily affected by eruptions in the middle and high latitudes. This paper analyzes the relationship between tree growth and volcanic activity but does not consider the influence of the type and timing of eruptions. We hope to shed more light on these factors in the future.

Compliance with ethical standards

References

Adams JB, Mann ME, Ammann C (2003) Proxy evidence for an El Niño-like response to volcanic forcing. Nature 426(6964):274–278

Brauning A, Mantwill B (2004) Summer temperature and summer monsoon history on the Tibetan plateau during the last 400 years recorded by tree rings. Geophys Res Lett 31(24)

Briffa KR, Jones PD, Schweingruber FH (1992) Tree-ring density reconstructions of summer temperature patterns across Western North America since 1600. J Clim 5(7):735–754

Briffa KR, Jones PD, Schweingruber FH, Osborn TJ (1998) Influence of volcanic eruptions on northern hemisphere summer temperature over the past 600 years. Nature 393(6684):450–455

Briffa KR, Osborn TJ, Schweingruber FH, Harris L, Jones PD, Shiyatov SG, Vaganov EA (2001) Low-frequency temperature variations from a northern tree ring density network. J Geophys Res 106(D3):2929–2941. https://doi.org/10.1029/2000JD900617

Cai QF, Liu Y, Tian H (2013) A dendroclimatic reconstruction of May–June mean temperature variation in the Heng Mounatins, north China, since 1767 AD. Quat Int 3–10

Chen F, Yuan YJ, Wei WS, Wang L, Yu SL, Zhang RB, Fan ZA, Shang HM, Zhang TW, Li Y (2012) Tree ring density-based summer temperature reconstruction for Zajsan Lake area, East Kazakhstan. Int J Climatol 32(7):1089–1097

Chen F, Yuan YJ, Chen FH, Wei WS, Yu SL, Chen XJ, Fan ZA, Zhang RB, Zhang TW, Shang HM, Qin L (2013) A 426-year drought history for western tian shan, central asia, inferred from tree rings and linkages to the north atlantic and indo-west pacific oceans. The Holocene 23(8):1095–1104

Chen F, Yuan YJ, Wei WS, Yu SL, Zhang TW, Shang HM, Zhang RB, Qin L, Fan Z (2015) Tree-ring recorded hydroclimatic change in Tienshan mountains during the past 500 years. Quat Int 358:35–41

Chen YN, Li WH, Deng HJ, Fang GH, Li Z (2016a) Changes in Central Asia's water tower: past, present and future. Sci Rep 6(1)

Chen F, Yu SL, He Q, Zhang RB, Kobuliev ZV, Mamadjonov YM (2016b) Comparison of drought signals in tree-ring width records of juniper trees from central and West Asia during the last four centuries. Arab J Geosci 9(4)

Chen F, Shang HM, Yuan YJ (2016c) Dry/wet variations in the eastern Tien Shan (China) since AD 1725 based on Schrenk spruce (Picea schrenkiana Fisch. et Mey) tree rings. Dendrochronologia 110–116. https://doi.org/10.1016/j.dendro.2016.07.003

Chen F, Yuan YJ, Wei WS, Yu SL, Shang HM, Zhang TW, Zhang RB, Wang HQ (2017) Air temperature from may through august in northern xinjiang reconstructed from multi-site tree-ring density. J Glaciol Geocryol (in Chinese, with English abstract)

Chen F, Yuan YJ, Yu SL, Chen FH (2019) A 391-year summer temperature reconstruction of the Tien Shan, reveals far-reaching summer temperature signals over the midlatitude Eurasian continent. J Geophys Res Atmos 124(22):11850–11862

Chenoweth M (2001) Two major volcanic cooling episodes derived from global marine air temperature, AD 1807-1827. Geophys Res Lett 28(15):2963–2966

Cook ER, Kairiukstis LA (1990) Methods of dendrochronology || some historical background on dendrochronology. Springer, Netherlands

Cook ER, Krusic PJ (2007) Program ARSTAN: a tree-ring standardization program based on detrending and autoregressive time series modeling, with interactive graphics. Lamont-Doherty Earth Observatory, Columbia University, Palisades, New York

Cook ER, D'Arrigo R, Mann ME (2002) A well-verified, multiproxy reconstruction of the Winter North Atlantic Oscillation Index since a.d. 1400*. J Clim 15(13):1754–1764

D'Arrigo R, Jacoby GC (1999) Northern North American tree-ring evidence for regional temperature changes after major volcanic events. Clim Chang 41(1):1–15

D'Arrigo R, Mashig E, Frank D, Wilson R, Jacoby GC (2005) Temperature variability over the past millennium inferred from northwestern Alaska tree rings. Clim Dyn 24(2):227–236. https://doi.org/10.1007/s00382-004-0502-1

D'Arrigo R, Wilson R, Anchukaitis KJ (2013) Volcanic cooling signal in tree ring temperature records for the past millennium. J Geophys Res 118(16):9000–9010

Dai AG, Trenberth KE, Qian T (2004) A global data set of Palmer Drought Severity Index for 1870–2002: relationship with soil moisture and effects of surface warming. J Hydrometeorol 5:1117–1130

Esper J, Schneider L, Krusic PJ, Luterbacher J, Buntgen U, Timonen M, Sirocko F, Zorita E (2013) European summer temperature response to annually dated volcanic eruptions over the past nine centuries. Bull Volcanol 75(7)

Fritts HC (1976) Tree rings and climate || Dendrochronology and Dendroclimatology. 1–54. https://doi.org/10.1016/B978-0-12-268450-0.50006-9

Fu CB, Zeng ZM (2005) Correlations between North Atlantic oscillation index in winter and eastern China flood/drought index in summer in the last 530 years. Sci Bull 50(21):2505–2516

Gray WM (1998) The Atlantic Ocean thermohaline circulation as a driver for multi-decadal variations in EL Nino intensity and frequency. In: Proceedings of the twenty-third annual climate diagnostics and predication workshop, 54–57

Hao XM, Li C, Li WH, Zhao RF (2011) Response of climate and hydrology change to North Atlantic oscillation and arctic oscillation in the west of northern Xinjiang during the last fifty years. J Desert Res (in Chinese, with English abstract)

Holder R, Mosteller F, Tukey JW (1979) Data analysis and regression. Appl Stat 28(2):177–178

Holmes RL (1983) Computer-assisted quality control in tree-ring dating and measurement. Tree-Ring Bull

Houghton JT (2004) Climate change in 1994: radiative forcing of climate change and an evaluation of the IPCC is92 emission scenarios. Cell Immunol 6(1):59–65

Huang R, Zhu HF, Liang EY, Asad F, Grieinger J (2019) A tree-ring-based summer (June-July) minimum temperature reconstruction for the western kunlun mountains since ad 1681. Theoretical and Applied Climatology 138(1–2):673–682. https://doi.org/10.1007/s00704-019-02849-1

Hughes MK, Schweingruber FH, Cartwright D, Kelly PM (1984) July-August temperature at Edinburgh between 1721 and 1975 from tree-ring density and width data. Nature 308(5957):341–344

Hurrell JW (1995) Decadal trends in the North Atlantic Oscillation: regional temperatures and precipitation. Science 269(5224):676–679. https://doi.org/10.1126/science.269.5224.676

Hurrell JW (1996) Influence of variations in extratropical wintertime teleconnections on northern hemisphere temperature. Geophys Res Lett 23(6):665–668

Hurrell JW, Loon HV (1997) Decadal variations in climate associated with the North Atlantic Oscillation. Clim Chang 36(3):301–326

IPCC (2013) In: Stocker, TF, Qin, DH, Plattner, G-K, Tignor, M, Allen, SK., Boschung, J, Nauels, A, Xia, Y, Bex, V, Midgley, PM (Eds.), Climate Change 2013: the Physical Science Basis. Contribution of Working Group I to the Fifth Assessment Report of the Intergovernmental Panel on Climate Change. Cambridge University Press, Cambridge, United Kingdom and New York, NY, USA

Jia PQ (2001) Study on the effects of volcanic eruption and solar activity on climate in China in recent 50 years. Plateau Meteorol

Jiang SX, Yuan YJ, Wei WS, Shang HM, Zhang TW, Zhang RB, Qin L (2016) Early summer temperature history in the Altay Mountains recorded by tree rings during 1579–2009. J Desert Res 36(4):1126–1132 (in Chinese, with English abstract)

Jiao L, Jiang Y, Wang MC, Kang XY, Zhang WT, Zhang LG, Zhao SD (2016) Responses to climate change in radial growth of Picea schrenkiana along elevations of the eastern Tianshan Mountains, Northwest China. Dendrochronologia 40:117–127. https://doi.org/10.1016/j.dendro.2016.09.002

Joel M (1987) Cross-validation in statistical climate forecast models. J Appl Meteorol 26(11):1589–1600

Jones PD, Jonsson T, Wheeler D (1997) Extension to the North Atlantic oscillation using early instrumental pressure observations from Gibraltar and south-west Iceland. Int J Climatol 17(13):1433–1450

Liang EY, Eckstein D, Shao XM (2009) Seasonal cambial activity of relict chinese pine at the northern limit of its natural distribution in North China-exploratory results. IAWA J 30(4):371–378

Liu Y (2006) Precipitation variation in the northeastern Tibetan plateau recorded by the tree rings since 850 ad and its relevance to the northern hemisphere temperature. Sci China 4(49):408–420

Liu Y, An ZS, Linderholm HW, Chen DL, Song HM, Cai QF, Sun JY, Tian H (2009) Annual temperatures during the last 2485 years in the mid-eastern Tibetan Plateau inferred from tree rings. Sci China Ser D Earth Sci 52(3):348–359

Liu J, Wang B, Cane MA, Yim SY, Lee JY (2013) Divergent global precipitation changes induced by natural versus anthropogenic forcing. Nature 493(7434):656–659

Man W, Zhou TJ, Jungclaus JH (2014) Effects of large volcanic eruptions on global summer climate and East Asian monsoon changes during the last millennium: analysis of MPI-ESM simulations. J Clim 27(19):7394–7409

Matsikaris A, Widmann M, Jungclaus JH (2016) Assimilating continental mean temperatures to reconstruct the climate of the Late Pre-industrial Period. Clim Dyn 46(11):3547–3566

Miller GH, Geirsdottir A, Zhong Y, Larsen DJ, Ottobliesner BL, Holland MM, Thordarson T (2012) Abrupt onset of the Little Ice Age

triggered by volcanism and sustained by sea-ice/ocean feedbacks. Geophys Res Lett 39(2):1–5. https://doi.org/10.1029/2011GL050168

Ning L, Liu J, Wang Z, Bradley RS (2018) Different influences on the tropical Pacific SST gradient from natural and anthropogenic forcing. Int J Climatol 38(4):2015–2028

Rayner NA, Parker DE, Horton EB, Folland CK, Alexander LV, Rowell DP, Kaplan A (2003) Global analyses of sea surface temperature, sea ice, and night marine air temperature since the late nineteenth century. J Geophys Res 108

Robertson AW, Mechoso CR, Kim Y (2000) The influence of Atlantic Sea surface temperature anomalies on the North Atlantic Oscillation. J Clim 13(1):122–138

Robock A (2000) Volcanic eruptions and climate. Rev Geophys 38(2):191–219

Robock A, Mao JP (1992) Winter warming from large volcanic eruptions. Geophys Res Lett 19(24):2405–2408

Rodwell MJ, Rowell DP, Folland CK (1999) Oceanic forcing of the wintertime North Atlantic oscillation and European climate. Nature 398(6725):320–323

Schmidt A, Ostro B, Carslaw KS, Wilson M, Thordarson T, Mann GW, Simmons AJ (2011) Excess mortality in Europe following a future Laki-style Icelandic eruption. Proc Natl Acad Sci U S A 108(38):15710–15715

Schoennagel T, Veblen TT, Romme WH, Sibold JS, Cook ER (2005) ENSO and PDO variability affect drought-induced fire occurrence in rocky mountain subalpine forests. Ecol Appl 15(6):2000–2014

Schweingruber FH, Fritts HC, Braker OU, Drew LG, Schar E (1978) The X-ray technique as applied to dendroclimatology. Tree-Ring Bull

Seddon AWR, Macias-Fauria M, Long PR, Benz D, Willis KJ (2016) Sensitivity of global terrestrial ecosystems to climate variability. Nature (advance online publication) 7593:229

Seim A, Tulyaganov T, Omurova G, Nikolyai L, Linderholm HW (2015) Dendroclimatological potential of three juniper species from the Turkestan range, northwestern Pamir-Alay Mountains, Uzbekistan. Trees 39(3):1–16

Shang HM, Wei WS, Yuan YJ, Yu SL, Chen X, Zhang TW, Liu XH (2010) The 150-year precipitation change recorded by tree ring in the central Tianshan Mountains. Arid Zone Res 27(3):443–449 (in Chinese, with English abstract)

Shang HM, Wei WS, Yuan YJ, Yu SL, Zhang TW, Zhang RB (2011) Early summer temperature history in northeastern Kazakhstan during the last 310 years recorded by tree rings. J Mt Sci 29:402–408 (in Chinese, with English abstract)

Shi F, Yang B, Feng J, Li JP, Yang FM, Guo ZT (2015) Reconstruction of the Northern Hemisphere annual temperature change over the common era derived from tree rings. Quat Sci 35(5):1051–1063 (in Chinese, with English abstract)

Splechtna BE, Dobrys J, Klinka K (2000) Tree-ring characteristics of subalpine fir (Abies lasiocarpa (Hook.) Nutt.) in relation to elevation and climatic fluctuations. Ann For Sci 57:89–100

Steinman BA, Mann ME, Miller SK (2015) Atlantic and Pacific multidecadal oscillations and Northern Hemisphere temperatures. Science 347(6225):988–991

Trouet V, Oldenborgh GJ (2013) Research tools knmi climate explorer: a web-based research tool for high-resolution paleoclimatology. Tree-Ring Res 69(1):3–13. https://doi.org/10.3959/1536-1098-69.1.3

Trouet V, Esper J, Graham NE, Baker A, Scourse JD, Frank D (2009) Persistent positive North Atlantic Oscillation mode dominated the Medieval climate anomaly. Science 324(5923):78–80

Wigley TML, Jones PD, Briffa KR (1987) Cross-dating methods in dendrochronology. J Archaeol Sci 14(1):51–64. https://doi.org/10.1016/S0305-4403(87)80005-5

Xin XG, Yu RC, Zhou TJ, Wang B (2006) Drought in late spring of South China in recent decades. J Clim 19(13):3197–3206

Yuan YJ, Shao XM, Li JF, Li XJ, Tang FL (2002) Discussion of precipitation information in Xiagansate tree-ring chronology and 326 year precipitation reconstruction. Acta Ecol Sin 22(12):2048–2053 (in Chinese, with English abstract)

Zhang QB, Cheng GD, Yao TD, Kang XC, Huang JG (2003) A 2,326-year tree-ring record of climate variability on the northeastern Qinghai-Tibetan Plateau. Geophys Res Lett 30

Zhang TW, Yuan YJ, Chen XJ, Fan ZA, Yu SL, Chen F, Shang HM, Zhang RB, Qin L (2015) Tree-ring-width based precipitation for the Mulei region in the East Tianshan Mountains. Quat Sci 35(5):1121–1133 (in Chinese, with English abstract)

Zhang RB, Yuan YJ, Wei WS, Gou XH, He Q, Shang HM, Zhang TW, Chen F, Bakytbek E, Yu SL, Qin L, Fan ZA (2016a) Tree-ring-based moisture variability in western Tianshan Mountains since A.D. 1882 and its possible driving mechanism. Agric For Meteorol 218-219:267–276. https://doi.org/10.1016/j.agrformet.2015.12.067

Zhang RB, Yuan YJ, Gou XH, Zhang TW, Zou C, Ji CR, Fan ZJ, Qin L, Shang HM, Li X (2016b) Intra-annual radial growth of Schrenk spruce (Picea schrenkiana Fisch. et Mey) and its response to climate on the northern slopes of the Tianshan Mountains. Dendrochronologia 36–42. https://doi.org/10.1016/j.dendro.2016.06.002

Zhang RB, Zhang TW, Kelgenbayev N, He Q, Maisupova B, Mambetov BT, Chen F, Dosmanbetov D, Shang HM, Yu SL, Yuan YJ (2017a) A 189-year tree-ring record of drought for the Dzungarian Alatau, arid Central Asia. J Asian Earth Sci 148:305–314. https://doi.org/10.1016/j.jseaes.2017.05.003

Zhang RB, Shang HM, Yu SL, He Q, Yuan YJ, Bolatov K, Mambetov BT (2017b) Tree-ring-based precipitation reconstruction in southern Kazakhstan, reveals drought variability since A.D. 1770. Int J Climatol 37(2):741–750

Zhang RB, Wei WS, Shang HM, Yu SL, Gou XH, Qin L, Boatov K, Mambetov BT (2019) A tree ring-based record of annual mass balance changes for the TS. Tuyuksuyskiy Glacier and its linkages to climate change in the Tianshan Mountains. Quat Sci Rev 10–21

Zhang RB, Qin L, Shang HM, Yu SL, Gou XH, Mambetov BT, Bolatov K, Zhang WJ, Ainur U, Bolatova A (2020) Climatic change in southern Kazakhstan since 1850 C.E. inferred from tree rings. Int J Biometeorol 64(5):841–851

Zhu HF, Shao XM, Yin ZY, Xu P, Xu Y, Tian H (2011) August temperature variability in the southeastern Tibetan Plateau since AD 1385 inferred from tree rings. Palaeogeogr Palaeoclimatol Palaeoecol 305(1):84–92. https://doi.org/10.1016/j.palaeo.2011.02.017